Journal of Energy Storage 32 (2020) 101741

Contents lists available at ScienceDirect

Journal of Energy Storage

journal homepage: www.elsevier.com/locate/est

A novel deep learning framework for state of health estimation of lithium-ion battery

Yaxiang Fan, Fei Xiao*, Chaoran Li, Guorun Yang, Xin Tang

National Key Laboratory of Science and Technology on Vessel Integrated Power System, Naval University of Engineering, 717 Jiefang Avenue, 430033, China

ARTICLE INFO

Keywords:
lithium-ion battery
State-of-health
Charging curve
Deep learning
Gated recurrent unit
Convolutional neural network, Hybrid network

ABSTRACT

The state-of-health (SOH) estimation is a challenging task for lithium-ion battery, which contribute significantly to maximize the performance of battery-powered systems and guide the battery replacement. The complexity of degeneration mechanism enables data-driven methods to replace mechanism modeling methods to estimate SOH. The insight that motivates this study is that the charging curve of constant current-constant voltage charging mode could reflect the magnitude of SOH from the perspective of capacity. The proposed approach is based on a hybrid neural network called gate recurrent unit-convolutional neural network (GRU-CNN), which can learn the shared information and time dependencies of the charging curve with deep learning technology. Then the SOH could be estimated with the new observed charging curves such as voltage, current and temperature. The approach is demonstrated on the public NASA Randomized Battery Usage dataset and Oxford Battery Degradation dataset, and the maximum estimation error is limited to within 4.3%, thus proving its effectiveness.

1. Introduction

Energy storage systems play a crucial role in a variety of industrial applications such as Electric Vehicles (EVs), Uninterruptible Power Supply (UPS), and renewable energy systems [1,13,14]. Due to their high energy density, high power density, strong environmental adaptability and low self-discharge rate, Lithium-ion batteries [2–6] are widely used in energy storage systems. To ensure the security and efficiency of battery operations, a battery management system (BMS) with the function of state estimation, battery equalization, safety control, and thermal management is essential. Among the functions of the BMS, the key issue is to estimate the state of charge (SOC) [7–9,19,20] and State of Health (SOH) [3,11,12].

SOH is a measure of the battery lifespan and reflects the reliability of the Li-ion battery relative to new battery. The lifespan degradation mechanism of lithium-ion battery is a very complicated process, which is affected by many factors such as charge and discharge rate, storage temperature, and usage. Compared with SOC estimation, SOH estimation is more challenging [10]. In practical applications, battery degradation can cause the change of the capacity and the internal resistance. Therefore, the SOH is often defined as a percentage that reflects the capacity fade and the power fade (internal resistance increase) as below.

$$\mathrm{SOH}=\frac{C_{now}}{C_0}\times 100\% \tag{1}$$

$$\mathrm{SOH}=\frac{R_{\mathrm{EOL}}-R_{\mathrm{now}}}{R_{\mathrm{EOL}}-R_{\mathrm{new}}}\times 100\% \tag{2}$$

where C_{now} represents the maximum allowable discharge capacity, C_0represents the nominal capacity of the battery, R_{now} represents the internal resistance at current time, R_{new} represents the internal resistance at current time from new cell, R_{EOL} represents the internal resistance at the battery's end-of-life.

In order to estimate the SOH of battery accurately and robustly, a variety of methods have been proposed. It mainly includes direct measurement method, model-based method and data-driven method [3]. The direct measurement method directly measure the capacity and the internal resistance in a test lab environment with the coulomb counting method [11], the open-circuit voltage (OCV) method [12], and internal resistance-based estimation method [15], and then obtain SOH according to Eq. (1) and Eq. (2). Although the direct measurement method is applicable to various batteries and easy to be implemented in BMS, but the estimation accuracy is highly dependent on the measurement technique. Besides, this method is only applicable for off-line estimation of SOH under test lab environment. The model-based method model the lithium-ion battery as an electrochemical model [16,17,21] or an electrical model [18,40–42] with prior knowledge.

* Corresponding author.
E-mail address: xfeyninger@gmail.com (F. Xiao).

https://doi.org/10.1016/j.est.2020.101741
Received 10 June 2020; Received in revised form 31 July 2020; Accepted 2 August 2020
Available online 10 August 2020

Then the model parameters include the aging characteristics of the lithium ion battery are identified by the least squares method [18] or the observer method, and then the SOH estimation is realized with the model parameters. However, it is difficult for choosing the right model to attain a trade-off between SOH estimation accuracy and the computational complexity, which limits its application in practice. Without considering the aging mechanism and internal electrochemical reaction of lithium-ion battery, the data-driven methods try to extract available features of battery degradation from the battery characterization data and then then establish the relationship between these features and SOH by machine learning methods. For example, cycle number [2], incremental capacity [22] and differential voltage [23] and candidate features in the voltage response under the current pulse test [24] are chose as the features to describe the battery degradation. Then the machine learning methods such as Support Vector Machine (SVM) [24], Gaussian Process Regression (GPR) [25], Grey Relational Analysis [22] and artificial neural networks (ANN) [2,2] are used to learn to the nonlinear mapping from features to SOH.

Although the data-driven researches mentioned above have achieved good estimation results under specific working conditions, there are still two critical problems should be considered. First, a significant limitation of the existing features extracted from the charging and discharging curve data is that a lot of details are missing. For example, the cycle number feature and the differential voltage feature ignore the working conditions of the battery. Besides, the feature extraction process is manual and requires significant domain expertise, which would bring extra consumption of manpower. The second problem is to choose the best machine learning algorithm to estimate the estimation model. Recently, deep learning technology such as deep neural network (DNN), convolutional neural network (CNN) and recurrent neural network (RNN) has been employed for in natural language processing, time series forecasting and system modeling. Compared with traditional machine learning method, the deep learning technology uses multiple layers to progressively extract higher level features from the raw input, which is able to eliminate of the need for feature engineering and the need for data labeling. Motivated by the successful application of deep learning, researchers began to employ it to battery state estimation. In [26] and [27], Ephrem et al. proposed a long short-term memory recurrent neural network (LSTM-RNN) and a CNN for the battery state of charge (SOC) estimation. Similarly, to overcome the short term dependence problem of simple RNN, [27] used the LSTM-RNN to synthesize a data-driven battery RUL predictor. Recently, Li et al. [2] presented an empirical model decomposition algorithm to extract high- and low-frequency features from cycle number data, and then the LSTM-RNN and Elman neural networks are established to predict high- and low-frequency sub-layers, respectively.

Different from these methods mentioned above, a novel battery SOH estimation approach is proposed based on the deep learning technology. The key idea behind our method is that the charging curve of constant current-constant voltage charging mode is able to reflect the magnitude of SOH from the perspective of capacity. Our method is based on a hybrid network called gate recurrent unit-convolutional neural network (GRU-CNN) [28,29], which is the augmentation of CNN with long GRU-RNN sub-modules. The convolutional block of CNN utilizes the shared weights structure to reduce the amount of weights and try to find the shared information from the measured voltage, current and temperature of charging data. For another, the GRU-RNN block uses their internal state (memory) to learn features and time dependencies from the sequential data. In fact, the combined structure could take advantages of both the CNN and GRU-RNN networks, and captures both shared spatial and temporal features of the charging data. The NASA dataset [30] and Oxford dataset [31] are used to demonstrate the effectiveness of the proposed method.

The rest of this paper is organized as follows: Section 2 presented the battery degradation data, and analyzed the relationship between the charging curves and SOH. Then the detail of GRU-CNN SOH estimation method is described in Section 3. Experimental evaluation is given in Section 4. Finally, Section 5 concludes the paper.

2. Datasets and features for SOH estimation

In this section, by analyzing the degradation characteristics of lithium-ion batteries from two public degradation datasets, the observable variables such as voltage, current and temperature of the charging curve are selected for SOH estimation.

The first one is the Randomized Battery Usage dataset (referred to simply as NASA dataset) [30] collected by NASA Ames Prognostics Center of Excellence (PCoE). The tests were conducted with 2.1-Ah, 4.2-V LG Chem. 18650 Li-cobalt cells produced by Idaho National Laboratory under randomized load profiles. The test equipment included a host computer, a battery cycler and a thermal chamber. 28 battery cells were divided into 7 groups of 4 and each group of cells under-went a different loading procedure such as different types of randomized currents and temperature. The voltage, current, capacity and cell temperature were recorded. The charging curves are obtained periodically every 50 random cycles or every 5 days by recording the constant-current-constant-voltage (CC-CV) charging protocol between the cell voltage limits. More detailed description could be found in Ref. [30].

Another dataset is the Oxford Battery Degradation dataset (referred to simply as Oxford dataset) [31] collected by DES, University of Oxford. 8 Kokam pouch cells of 740 mAh nominal capacity and 4.2 V nominal voltage are tested under ARTEMIS urban drive cycle. The thermal chamber is set to 40°C, and the cell are repeated charging and discharging process with constant current until the capacity reaches about 80% of the nominal capacity. Similar as the NASA dataset, the charging curves (include the voltage, current, capacity and cell temperature) are obtained every 100 cycles by recording the constant-current (CC) charging protocol between the cell voltage limits.

From the two public degradation datasets, it is obvious to observe that the charge process is peaceable compared to the discharge process. This is due to the reason that the former is controllable to battery management system. Consequently, the external and internal parameters in the CC-CV charge process shows certain regularities with capacity. As shown in Fig. 1, the voltage rise slower and the charging current remain constant for a longer time with larger SOH. On the contrary, when the battery performance deteriorate (SOH decrease), the contrary phenomenon can be observed. This is mainly because the battery under different SOH would have different internal property and external performance, and then lead to the discriminant voltages and curve shapes as mentioned above. Besides, we can observe the similar rule from the voltage and SOH curves with time of Cell 6# in Oxford dataset in Fig. 2. It's worth noting that the charging current and temperature are not provided for the reason that they are constant in the Oxford dataset.

Inspired by these facts, plenty of works try to extract features such as cycle number [2], incremental capacity [22] and differential voltage [23] and candidate features in the voltage response from the charging curve. Different with these methods mentioned above, in this paper we proposed to directly utilize the charging curves as the feature to estimate SOH with the advantage of more details and need not the artificial feature extraction.

3. Methodologies

3.1. Problem formulation

Given a training set of pairs $\mathcal{D} = \{(x_i, y_i)\}_{i=1}^{N_D}$, the goal of data-driven based SOH estimation problem is to learn the nonlinear mapping $f(\bullet)$ from the observed quantities x to SOH y, where the x is the voltage, current and temperature of charging curves and N_D is the number of training examples. Then the SOH y' could be estimated with its charging curves x' and the the nonlinear mapping $f(\bullet)$ as below.

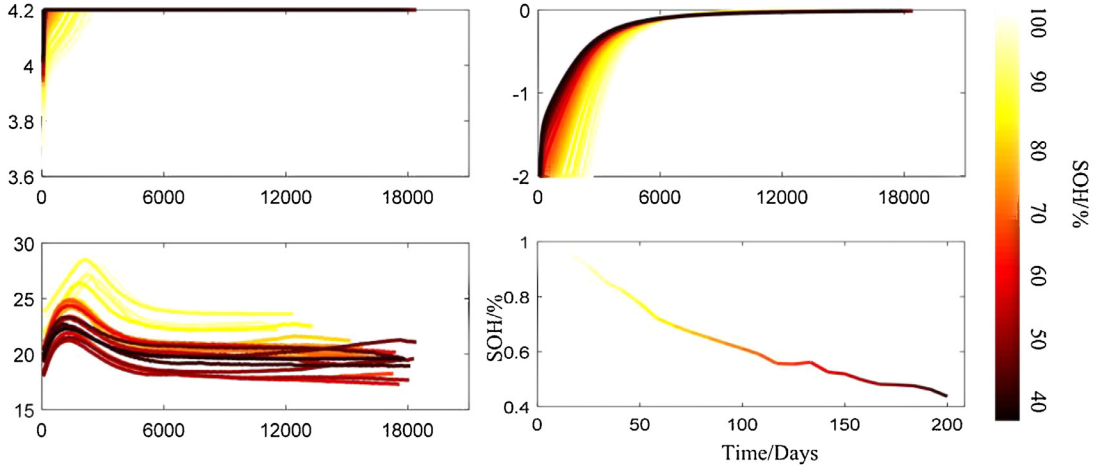

Fig. 1. Voltage, current, temperature and SOH curves with time of RW15 in NASA dataset.

$$y' = f(x') \tag{3}$$

In this paper we introduce a hybird neural network called the GRU-CNN network to learn the nonlineat mapping $f(\bullet)$ as shown in Fig. 4.

3.2. Gated recurrent unit recurrent neural network

Recurrent neural network [32] is one of the artificial neural networks (ANNs) that have the recurrent connections. It applies to the sequential tasks [35] such as learning temporal representations, modeling, recognizing and predicting the sequential data. In detail, the hidden states work as the memory of the network and the current state is jointly impacted by current input and the previous state. However, the RNN is the impractical at first because the long-term dependencies problem [33], which lead to gradients exploding and vanishing during back-propagation process for the long time series and complex hidden layers. To address these questions, gating mechanism such as gated recurrent unit (GRU) is proposed to control gradients information propagation. The GRU utilizes the reset gate $\mathbf{r}_t$ and update gate $\mathbf{z}_t$ to modulate the flow of information inside the unit. In detail, the update gate control the update of hidden state and the reset gate decide whether to ignore the previous hidden state. For a one-layer GRU-RNN, update gate, the reset gate, output candidate, and GRU output are calculated as follows:

$$z_t = \sigma(W_z x_t + U_z h_{t-1} + b_z) \tag{4}$$

$$r_t = \sigma(W_r x_t + U_r h_{t-1} + b_r) \tag{5}$$

$$\tilde{h}_t = \varphi(U(r_t \odot h_{t-1}) + W_c x_t + b_{\tilde{h}}) \tag{6}$$

$$h_t = z_t \odot h_{t-1} + (1 - z_t) \odot \tilde{h}_t \tag{7}$$

where $\odot$ represents an element-wise multiplication; W_z, W_r and W_c are the weight parameter; b_z, b_r and $b_{\tilde{h}}$ are the bias parameter; $\sigma(\cdot)$ is the gate activation function; $\varphi(\cdot)$ is the output activation function. The architecture detail of GRU-RNN are show in Fig. 3.

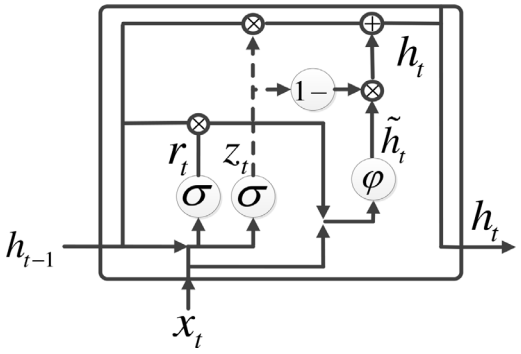

Fig. 3. The architecture detail of GRU-RNN.

3.3. Convolutional neural network

Convolutional neural network (CNN) have achieved achieve great success [35] in image and video recognition, natural language processing and time series classification. Different with the RNN, the CNN is one of the feedforward neural network (FNN). Actually, in the FNN the information moves in only one direction and it contains no recurrent connections. Inspired by receptive fields' theory from the biological processes [34], CNN utilizes the share convolving filters to extract the local features. This is due to the reason that the data have inherent dependencies between adjacent dimensions. The convolutional layers, pooling layer and dense layer are used in CNN to extract complex feature representations from the data, reduce the dimensions and predict the result, respectively. Above all, local connections, shared weights, pooling and the use of many layers constitutes the key to success of CNN.

In detail, the CNN is trained to learn the parameters Θ of a composite nonlinear function $F(x|\Theta)$ from the input x to the output y.

$$y = F(x|\Theta) = f_L(\cdots f_2(f_1(x|\theta_1)|\theta_2)|\theta_L) \tag{8}$$

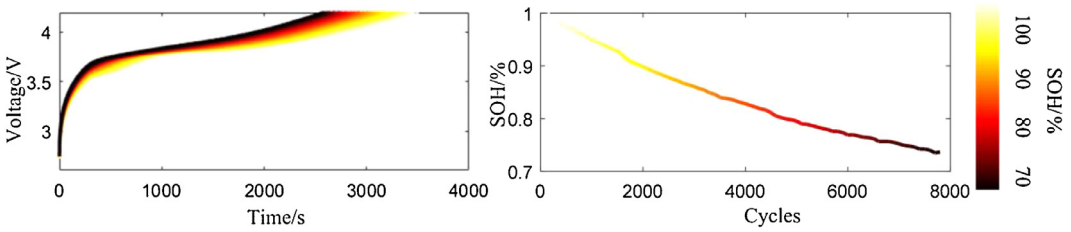

Fig. 2. Voltage and SOH curves with time of Cell 6# in Oxford dataset.

where each operation $f_l(x|\theta_l)$ is referred to as the convolutional layer, the pooling layer and the dense layer of the network and $\Theta = \{\theta_1, \theta_2, ..., \theta_L\}$. More specifically, the convolutional layer and the dense layer are expressed as (7) and (8), respectively.

$$y_l = f_l(x_l|\theta_l) = h(W_l * x_l + b_l),\ \theta_l = [W_l, b_l] \tag{9}$$

$$y_l = f_l(x_l|\theta_l) = h(W_l \cdot x_l + b_l),\ \theta_l = [W_l, b_l] \tag{10}$$

where W_l and b_l represent the filters and bias, * and $\cdot$ refer to a valid convolution and an element-wise multiplication.

3.4. SOH estimation based on gate recurrent unit-convolutional neural network

Both the GRU-RNN and CNN mentioned above have been applied to deal with the time series prediction problem. This is mainly because the two networks are able to find the shared information (extract feature) and mine the time dependencies from the sequential data, respectively. To take advantage of both networks mentioned above, we introduced a hybrid network called gate recurrent unit-convolutional neural network (GRU-CNN) to deal with the SOH prediction problem. As in [36–38], the similar hybrid network such as long short term memory fully convolutional network (LSTM-FCN) and Attention-BLSTM-RNNs with FCNs have been widely applied in time series classification and speech emotion recognition. The proposed architecture actual implementation is shown in Fig. 4. It is obvious that the architecture has two parallel streams: a GRU and a CNN. The CNN stream contains six temporal convolution blocks, which consists of a convolution layer, followed by batch normalization, followed by ReLU activation function. A flatten layer and a fully-connected (Dense) layer is followed at the end of the CNN for dimension conversion. On the other hand, it contains a gated recurrent unit (GRU) layer and a fully-connected (Dense) layer. At the end of the GRU-CNN architecture, the final output of the two streams are concatenated and projected to the output. At the end of each forward propagation, the loss function L of GRU-CNN is calculated as follows:

$$L = \frac{1}{n}\sum_{t=1}^{n} |y(t) - y(t)'| \tag{11}$$

where $y(t)$ and $y(t)'$ are the real value and estimated value for a particular charging curve t, respectively. n is the total number of the trainset.

Table 1
Specifications of The GRU-CNN architecture.

layer	input	kernel size	kernel number	output	last/ next layer
I0	3 × 256	N/A	N/A	3 × 256	N/A
C1	3 × 256	1 × 32	64	64 × 256	I0/P1
P1	64 × 256	1 × 2	N/A	64 × 128	C1/C2
C2	64 × 128	1 × 32	64	64 × 128	P1/P2
P2	64 × 128	1 × 2	N/A	64 × 64	C2/C3
C3	64 × 64	1 × 32	64	64 × 64	P2/P3
P3	64 × 64	1 × 2	1/0	64 × 32	C3/C4
C4	64 × 32	1 × 32	64	64 × 32	P3/P4
P4	64 × 32	1 × 2	N/A	64 × 16	C4/C5
C5	64 × 16	1 × 32	64	64 × 16	P4/P5
P5	64 × 16	1 × 2	N/A	64 × 8	C5/C6
C6	64 × 8	1 × 32	64	64 × 8	P5/P6
P6	64 × 8	1 × 2	1/0	64 × 4	C6/F1
F1	64 × 4	N/A	N/A	1 × 256	P6/D1
D1	1 × 256	N/A	64	1 × 64	F1/M1
G1	3 × 256	N/A	256	1 × 256	I0/D2
D2	1 × 256	N/A	64	1 × 64	G1/M1
M1	1 × 128	N/A	1	1	D1 + D2/ O0
O0	1	N/A	N/A	N/A	M1

I = input layer, C = convolutional layer, P = maxpooling layer, D = dense layer, M = concatenate layer, G = GRU layer, F = flatten layer, O = output layer

As the input of the GRU-CNN, the raw data of the fixed charge curves (voltage, current, temperature) have converted to fixed dimension $x(t) \in \mathbb{R}^{N\times M}$, where $x(t) = [I(t), V(t), T(t)]$ and $N = 256$ and $M = 3$. For the GRU-RNN stream, the number of hidden-layer nodes is set as 256 and the nodes of the fully-connected (Dense) layer is set as 64. And for the CNN stream, the convolution number and size of each convolution layer is set as 64 and 32 × 1. The detailed configurations of the whole network architecture are shown in Table 1. The experiments are conducted on a desktop with Intel Core i7-8700k 3.2GHz CPU, NVIDIA GeForce GTX 1070Ti (8 GB on-board memory) GPU and 16GB RAM. All models were trained using the Keras [32] library with the TensorFlow [33] backend. The parameters of the network were optimized using Adam optimizer [39] with a fixed learning rate of 0.00001, the first-order momentum attenuation coefficient β_1 of 0.9, the second-order momentum attenuation coefficient β_2 of 0.999, mini-batches of size 100 and total epoch of 10000.

The experiment procedure is shown in Fig. 5 and the entire

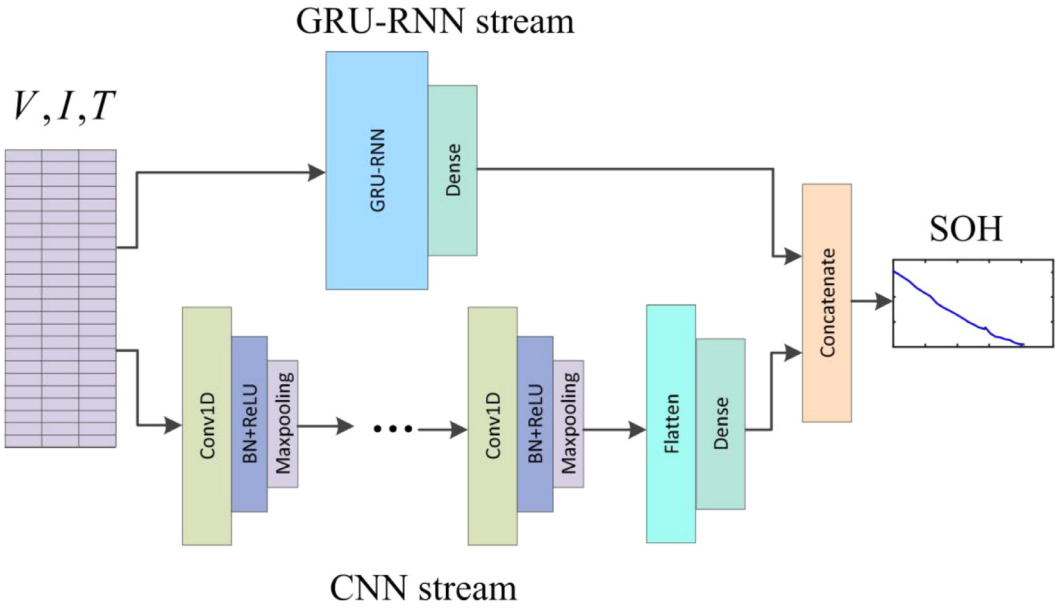

Fig. 4. The GRU-CNN architecture.

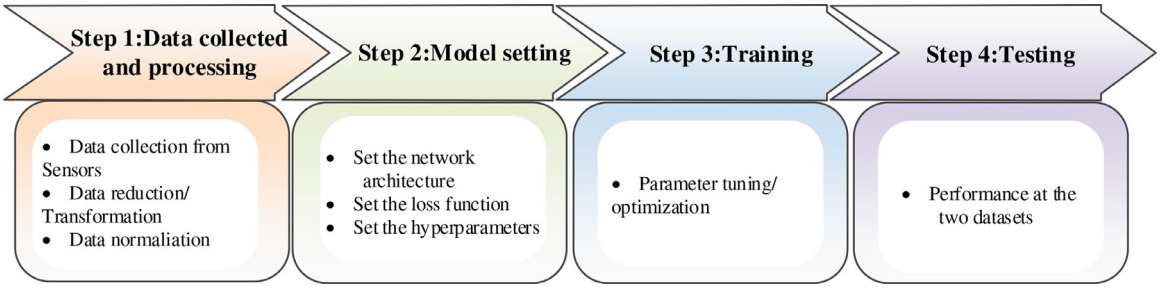

Fig. 5. The experiment procedure.

processes can be described as follows:

Step I: Obtain the charging data (voltage, current and temperature) from the sensors and convert the the entire charging data to 256 × 3 vector with the equally spaced resample method. Then normalize the data and split it into training data and testing data.

Step II: Set the numbers of input layer nodes, hidden layer nodes, and output layer nodes of the GRU-CNN; set the hyperparameters of the GRU-CNN including the timestep, sampling interval, batch size, and iteration; select the optimization algorithm and initialize the weights in the GRU-CNN.

Step III: Use the training data to learn the weights of GRU-CNN with the Adam optimizer.

Step IV: SOH estimation is conducted for the testing data to evaluate the performance of the proposed method with the trained GRU-CNN.

4. Results and discussions

4.1. Implementation details

Since the raw charging data are unequal length, they are processed to the fixed length with the resampling method to match the input size of the GRU-CNN. To avoid the problem of over-fitting in the training stage, we adopted the data augmentation technique. Specifically, based on the error range provided during the testing of the dataset, Gaussian noise with 0 mean and a standard deviation of 1-2% is injected into the voltage, current and temperature measurements. In addition, considering the inherent offset of the battery management system in actual measurement, an offset of up to ± 0.1V, ± 0.005A and ± 2.5°C is applied to the measured voltage, current and temperature, respectively. Then up to 65 augmented copies of training data are created for training. At the last, to remove the negative effect that improves the convergence rate, the data are normalized to the range [−1, 1].

To evaluate the accuracy of GRU-CNN for SOH estimation of battery, Mean Absolute Error (MAE) and Maximum Error (MAX) are used for evaluation criteria as below.

$$\mathrm{MAE} = \frac{1}{n}\sum_{t=1}^{n}|y(t) - y(t)'| \tag{12}$$

$$\mathrm{MAX} = \max|y(t) - y(t)'| \tag{13}$$

where $y(t)$ and $y(t)'$ are the real value and estimated value for a particular charging curve t, respectively. n is the total number of the trainset.

4.2. Experiment result on NASA dataset

For the NASA dataset, 28 cells data are divided into 7 different test groups according to the different loading procedure. To validate the completeness performance of the proposed method on different working condition, we select four cells data (RW 16#: 25°C, low-rate discharge; RW 20#: 25°C, high-rate discharge, RW 24#: 40°C, low-rate discharge, RW 28#: 40°C, high-rate discharge) as the testing set. And the rest 24 cells data are chose as the training set. To demonstrate the superiority of hybrid network, the estimation results of the two single streams are also provided for comparison. For each of the single stream, the concatenate layer is ignored and the output layer is followed at the end of the stream. Another two existing SOH estimation algorithms than based on the machine learning methods are introduced for comparison. One method is based the Support Vector Regression (SVR) [24] and the other method is based on the Gaussian Process Regression (GPR) [25]. In detail, the raw data of the fixed charge curves (voltage, current, temperature) have converted to fixed dimension as the input to used to learn to the non-linear mapping from charge curves to SOH with the SVR and GPR. The RBF kernel is adopted for the SVR method and the regularization parameter C and the gamma are set as 100 and 0.01. Besides, the GPR method adopted the squared exponential covariance (SE) function as the kernel function and the mean function is set as 0.

Fig. 6 shows the SOH estimation results and errors of battery RW 16#, 20#, 24# and 28#. It is clear that the SOH estimation curves of the three methods for all the four testing battery are very closed to the measured SOH curves. Besides, the red curve (GRU-CNN) has achieved the smallest estimation errors among the three methods. The quantitative results in form of MAE and MAX are presented in Table 2. From the Fig. 6, it can be noted that the SOH tends to degrade significantly with days. Clearly, the two batteries (RW 16# and RW 20#) working at the 40°C age much fasteter than the two data (RW 24# and RW 28#) since the former two data have fewer data points. By simple calculation with the results from Table 2, the overall MAE and MAX of SOH estimation results are 2.52%, 2.17%,1.51%, 1.78%, 1.03% and 17.04%, 9.61% 5.93%, 9.42%, 4.11% for the SVR, GPR, CNN, GRU and GRU-CNN method, respectively. Overall, the total performace of the three deep learning method are superior to the two machine learning methods. That may be due to the reason that the success of machine learning method depend on the feature engineering, which is not adopted for the our expeiment. The results further demonstrate that the deep learning methods could estimate accurate SOH depend on the raw charging curve without the feature engineering. In detail, it is clear that the performance of GRU-CNN is superior to both the CNN and GRU, with a MAE decrease of 31.8% and 42.1%, respectively. It should be pointed out either the shared weights or time dependencies is employed in the two cases. And the hybrid network centers the advantage of both the two single network. Another superiority of the proposed method is that no special requirement for battery discharge condition, since the proposed estimation method achieved the similar results for the four batteries of different working conditions.

4.3. Experiment result on oxford dataset

Compared with the NASA dataset, the working condition of the Oxford dataset is much simpler. In detail, the cells are repeated discharging process with 1C at 40°C. Only the voltage is taken as the input to the network for then reason that the current and temperature are constant in this dataset. Cell 4# and Cell8# are chose as the testing set and the rest 6 cells are taken as the training set. Same as the Section 4.2, the two machine learning method (SVR and GPR) and two deep learning method (CNN and GRU) are used for comparsion, to determine

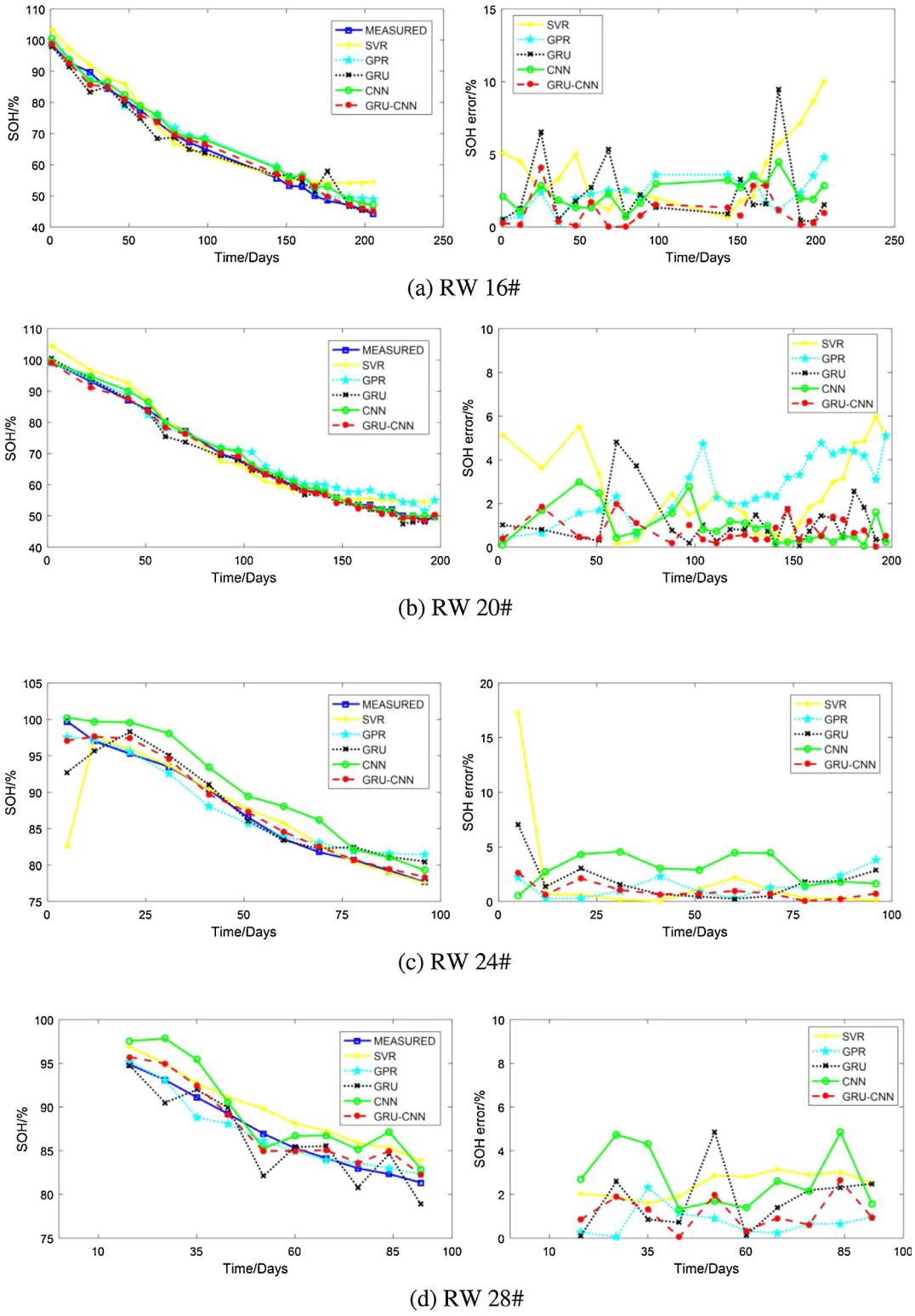

Fig. 6. Estimation accuracy and estimation error of the testing set for the NASA dataset. (a) RW 16#, (b) RW 20#, (c) RW 24#, (d) RW 28#.

if the proposed method can achieve the state-of-the-art accuracy in SOH estimations. The hyperparameters of the contrast method are chose the same as in the the Section 4.2. The estimated curves are shown in Fig. 7. and Table 5 summarizes the SOH estimation results.

From the Fig. 6, it can be noted that the SOH tends to degrade significantly with cycles. It can be observed that the SOH is accurately estimated for all the five methods with less than 5% MAE. Obviously, the SOH estimation results of the two machine learning methods underperformed to the results of the three deep learning methods. The results shown in Fig. 7 and Table 3, point to an overall MAE of 4.52%, 2.44%, 1.43%, 1.09% and 0.62% for the five methods, respectively. As can be seen from the Table 5, it is obvious that the performance of GRU-CNN superior than the two single network. In detail, the CNN method achieved the 1.24% MAE and 2.00% MAX for the Cell 4#, and 1.56% MAE and 2.77% MAX for the Cell 8#. The estimation result of GRU shows similar trend with real SOH curve but with larger oscillation of

Table 2
MAEs and MAXs of the SOH estimation results for the NASA dataset.

Battery number	Criteria	SVR	GPR	CNN	GRU	GRU-CNN
RW 16#	MAE(%)	3.84	2.34	1.38	2.34	1.07
	MAX(%)	9.71	9.61	4.87	9.42	4.11
RW 20#	MAE(%)	2.49	1.12	1.07	1.12	0.97
	MAX(%)	6.02	4.54	2.83	4.88	1.98
RW 24#	MAE(%)	2.19	1.93	2.32	1.93	0.95
	MAX(%)	17.04	7.21	4.79	6.94	2.64
RW 28#	MAE(%)	2.57	1.76	1.74	1.76	1.15
	MAX(%)	3.63	5.02	4.64	4.73	2.33
Overall	MAE(%)	2.52	2.17	1.51	1.78	1.03
	MAX(%)	17.04	9.61	5.39	9.42	4.11

more than 4% MAX. And for the GRU-CNN method, it achieved the 0.61% MAE and 1.60% MAX for the Cell 4#, and 0.65% MAE and 1.62% MAX for the Cell 8#. Compared with the results of the NASA dataset, it can be concluded that the proposed performs in general with more accuracy for the Oxford dataset. Here the reason is that the Oxford dataset is repeated charging and discharging process with constant current, which is less challenge than the NASA dataset.

4.4. Effect of different fixed length N

Since the raw charging data are unequal length, they are processed to the fixed length N with the resampling method to match the input size of the GRU-CNN. The number of fixed length N determines the available information for features and the total number of trainable parameters of deep learning models. Different numbers of fixed length N were constructed to assess the effect on estimation performance. The fixed length N is set as 64, 128, 256, 384, 512, and Fig. 8 are the estimation performance on the two datasets. Noted that the $N \geq 64 = 2^6$ for the reason that 6 pooling layers is adopted for our work.

As can be observed, both the MAE and MAX of the two datasets decreases with the number of fixed length N when $N \leq 256$. This can be attributed to the reason that low-dimensional data lose important information. However, the variation in estimation accuracy have made little difference when the timestep going from $N = 256$ to $N = 512$. As larger N leads to more trainable parameters of deep learning models and thus require more computation cost, thus $N = 256$ seems to be a reasonable choice by trading-off estimation accuracy against computational cost.

Table 3
MAEs and MAXs of the SOH estimation results for the Oxford dataset.

Battery number	Criteria	SVR	GPR	CNN	GRU	GRU-CNN
Cell 4#	MAE(%)	4.23	2.12	1.24	1.43	0.61
	MAX(%)	11.47	5.83	2.00	4.21	1.60
Cell 8#	MAE(%)	4.71	2.65	1.56	0.88	0.65
	MAX(%)	9.85	4.13	2.77	3.32	1.62
Overall	MAE(%)	4.52	2.44	1.43	1.09	0.62
	MAX(%)	11.47	5.83	2.77	4.21	1.62

4.5. Processing time

In this subsection, we provide the computational times of the proposed methods in form of the training time and testing for each dataset. As mentioned in the Section 3.4, all the experiments are conducted on a desktop with Intel Core i7-8700k 3.2GHz CPU, NVIDIA GeForce GTX 1070Ti (8 GB on-board memory) GPU and 16GB RAM. The three deep learning methods are implemented in Python 3.6.5 in combination with Keras 2.2.4, Tensorflow 1.7.0, Pandas 0.23.0 Scikit-learn 0.24.0 and Numpy 1.15.3. And for the two machine learning methods, they are implemented in Python 3.6.5 in combination with Scikit-learn 0.24.0, Pandas 0.23.0 and Numpy 1.15.3. Table 4 summarizes the mean computational times over the 10 runs.

It is not surprising to observe that the training time of the all the methods are more than 4000s except for the GPR which use inducing points for sparse regression [43]. Obviously, the proposed GRU-CNN

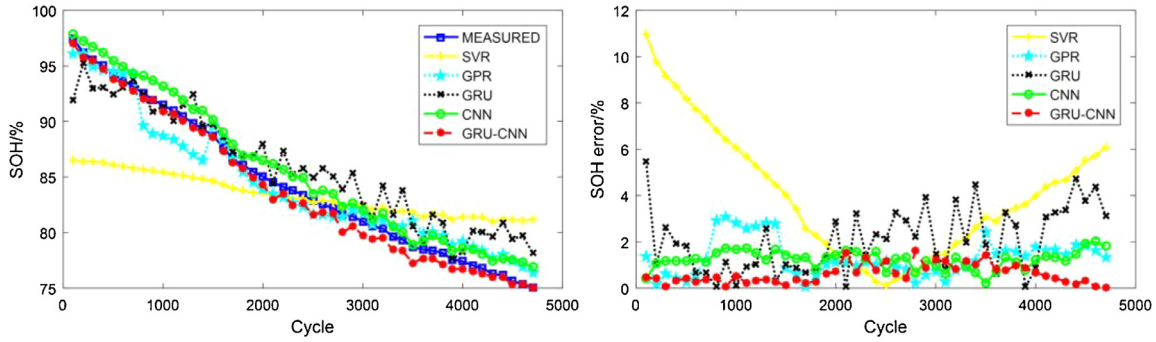

(a) Cell 4#

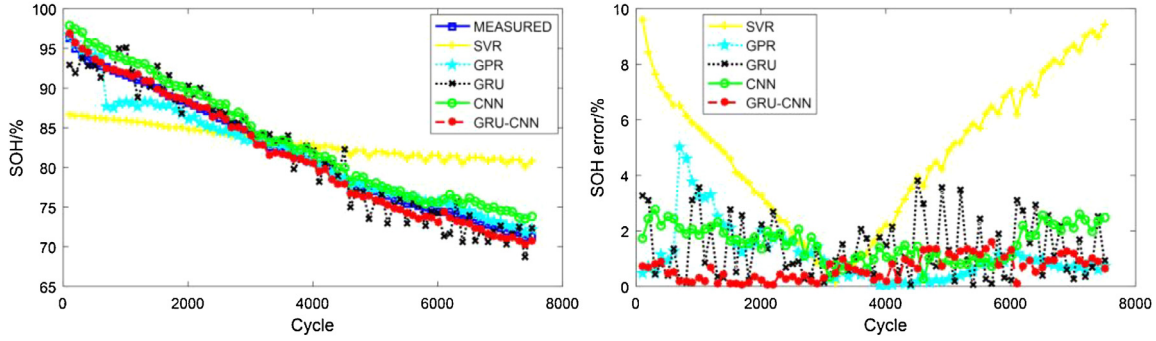

(b) Cell 8#

Fig. 7. SOH estimation results and errors of battery Cell 4# and Cell 8# for the Oxford dataset. (a) Cell 4#, (b) Cell 8#.

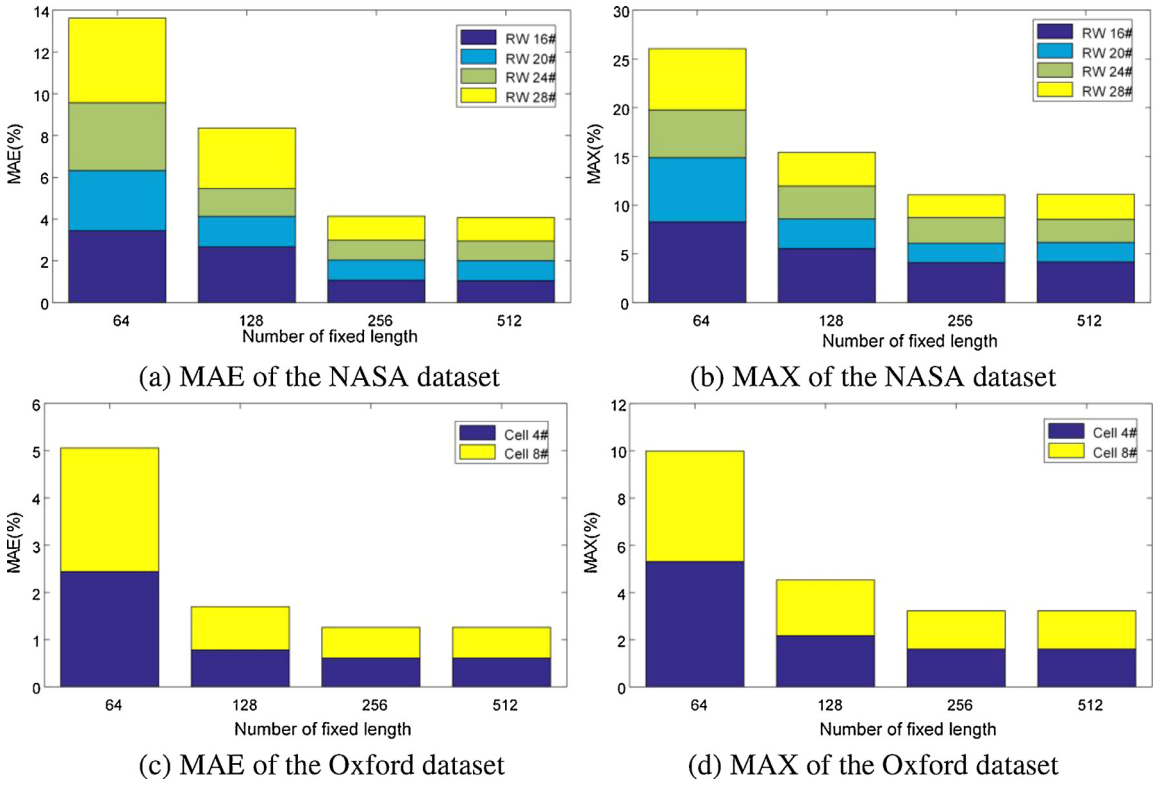

Fig. 8. Estimation accuracy measured versus the number of fixed length *N*. (a) MAE of the NASA dataset (b) MAX of the NASA dataset, (c) MAE of the Oxford dataset (d) MAX of the Oxford dataset.

and GRU spend much more training time than the CNN. This is due to the reason that the GRU unit has more complex structure and training the GRU unit is time consuming. However, all methods showed a short test time, which suggest that these data-driven methods can be implemented online.

5. Conclusions

In this paper we presented an effective approach for SOH estimation of lithium-ion battery based on deep learning technology. Our approach takes it as a time series prediction problem and builds upon the two stream hybrid network framework, which employed the GRU and CNN, respectively. In the training stage, the voltage, current and temperature of the charging curve and SOH are used as the input and output to learn the estimation model. In the testing stage, the SOH could be estimated with the new observed charging curves. Both the shared weights and time dependencies of the GRU and CNN are employed, and GRU-CNN with the best settings achieved overall MAXs as low as 4.11% for the NASA dataset and 1.62% for the Oxford dataset. Besides, the qualitative and quantitative results that our method is capable to precisely predict the SOH regardless of special requirement for battery discharge condition. The complex and time consuming feature extracting procedure is no longer need in the proposed method. The processing time compassion shows that the proposed method took less than 1s to estimate the SOH for the testing stage, which means the proposed method could be implemented online.

To extend this work, the future research will concentrate on applying the proposed method in the prototype hardware implementation such as AI chip for the BMS.

CRediT authorship contribution statement

Yaxiang Fan: Conceptualization, Methodology, Software, Investigation, Writing - original draft. **Fei Xiao:** Resources, Writing - review & editing, Supervision, Data curation. **Chaoran Li:** Validation, Formal analysis, Visualization, Software. **Guorun Yang:** Visualization. **Xin Tang:** Writing - review & editing.

Declaration of Competing Interest

The authors declared that they have no conflicts of interest to this work.

Acknowledgements

This research was funded by National Defense Science Innovation Zone Project and the National Natural Science Foundation of China (51907200).

Table 4
Execution time of our proposal method and the comparison methods.

Dataset		SVR	GPR	CNN	GRU	GRU-CNN
The NASA dataset	Training time (s)	10316.18	446.71	4237.71	57268.44	60193.27
	Testing time (s)	0.12	0.16	0.34	0.22	0.62
The Oxford dataset	Training time (s)	4912.51	319.14	1872.28	23862.13	26171.41
	Testing time (s)	0.07	0.11	0.26	0.15	0.46

References

[1] L. Zheng, L. Zhang, J. Zhu, et al., Coestimation of state-of-charge, capacity and resistance for Lithium-ion batteries based on a high-fidelity electrochemical model, Appl. Energy 180 (2016) 424–434.

[2] X. Lia, L. Zhang, Z. Wang, P. Dong, Remaining useful life prediction for lithium-ion batteries based on a hybrid model combining the long short-term memory and Elman neural networks, J. Energy Storage (2019) 510–518.

[3] H. Dai, G. Zhao, M. Lin, Ji Wu, G. Zheng, A novel estimation method for the state of health of lithium-ion battery using prior knowledge-based neural network and Markov chain, IEEE Trans. Indust. Electron. 60 (10) (2019) 7706–7716.

[4] Z. Wang, S. Zeng, J. Guo, T. Qin, State of health estimation of lithium-ion batteries based on the constant voltage charging curve, Energy 167 (2019) 661–669.

[5] J. Wei, G. Dong and Z. Chen. Remaining useful life prediction and state of health diagnosis for lithium-ion batteries using particle filter and support vector regression. IEEE Trans. Indust. Electron., 65, 7: 5634-5643.

[6] Y. Denga, H. Ying, J. Ea, H. Zhua, K. Wei, J. Chen, F. Zhang, G. Liao, Feature parameter extraction and intelligent estimation of the state-of-health of lithium-ion batteries, Energy 176 (1) (2019) 91–102.

[7] M. Ye, H. Guo, B. Cao, A model-based adaptive state of charge estimator for a lithium-ion battery using an improved adaptive particle filter, Appl. Energy 190 (2017) 740–748.

[8] B Xiong, J Zhao, Y Su, et al., State of charge estimation of vanadium redox flow battery based on sliding mode observer and dynamic model including capacity fading factor, IEEE Trans. Sustain. Energy 8 (4) (2017) 1658–1667.

[9] S. Tong, J.H. Lacap, J.W Park, Battery state of charge estimation using a load-classifying neural network, J. Energy Storage 7 (2016) 236–243.

[10] M. Berecibar, M. Germandia, I. Gandiage, et al., State of health estimation algorithm of LiFePO4 battery packs based on differential voltage curves for battery management system application, Energy 103 (2016) 784–796.

[11] W. He, N. Williard, C. Chen, et al., State of charge estimation for Li-ion batteries using neural network modeling and unscented Kalman Filter-based error cancellation, Electr. Power Energy Syst. 62 (2014) 783–791.

[12] L. Chen, Z.Q. Lü, W.L. Lin, H.H. Pan, A new state-of-health estimation method for lithium-ion batteries through the intrinsic relationship between ohmic internal resistance and capacity, Measurement 116 (2018) 586–595.

[13] Y. Wang, X. Li, L. Wang, Z. Sun, Multiple-grained velocity prediction and energy management strategy for hybrid propulsion systems, J. Energy Storage (26) (2019) 100950.

[14] Y. Wang, Z. Sun, Z. Chen, Energy management strategy for battery/ supercapacitor/ fuel cell hybrid source vehicles based on finite state machine, Appl. Energy (254) (2019) 113707.

[15] M. Galeotti, L. Cinà, C. Giammanco, et al., Performance analysis and SOH (state of health) evaluation of lithium polymer batteries through electrochemical impedance spectroscopy, Energy 89 (2015) 678–686.

[16] C.R. Birkl, E. McTurk, S. Zekoll, F.H. Richter, M.R. Roberts, P.G. Bruce, D.A. Howey, Degradation diagnostics for commercial lithium-ion cells tested at −10°C, J. Electrochem. Soc. 164 (12) (2017) 2644–2653.

[17] C.R. Birkl, M.R. Roberts, E. McTurk, P.G. Bruce, David A. Howey, Degradation diagnostics for lithium ion cells, J. Power Sourc. 341 (2017) 373–386.

[18] A. Downeya, Y. Luib, C. Hu, S. Laflamme, S. Hub, Physics-based prognostics of lithium-ion battery using non-linear least squares with dynamic bounds, Reliab. Eng. Syst. Saf. 182 (2019) 1–12.

[19] Y. Wang, C. Liu, R. Pan, Z. Chen, Modeling and state-of-charge prediction of lithium-ion battery and ultracapacitor hybrids with a co-estimator, Energy (121) (2017) 739–750.

[20] Y. Wang, C. Zhang, Z. Chen. A method for joint estimation of state-of-charge and available energy of LiFePO4 batteries. Appl. Energy, 135: 81-87.

[21] J. Li, K. Adewuyi, N. Lotfi, et al., A single particle model with chemical/mechanical degradation physics for lithium-ion battery state of health (SOH) estimation, Appl. Energy 212 (2018) 1178–1190.

[22] X. Li, Z. Wang, L. Zhang, C. Zou, D.D. Dorrelld, State-of-health estimation for Li-ion batteries by combing the incremental capacity analysis method with grey relational analysis, J. Power Sourc. 410 (15) (2019) 106–114.

[23] Y. Li, M.A. Monema, R. Gopalakrishnana, M. Berecibara, E. Nanini-Maury, N. Omara, P. v.d.Bosschea, J.V. Mierloa, A quick on-line state of health estimation method for Li-ion battery with incremental capacity curves processed by Gaussian filter, J. Power Sourc. 373 (2018) 40–53.

[24] J. Menga, L. Cai, G. Luo, D. Stroe, R. Teodorescu, Lithium-ion battery state of health estimation with short-term current pulse test and support vector machine, Microelectron. Reliab. 88–90 (2018) 1216–1220.

[25] D. Yang, X. Zhang, R. Pan, Y. Wang, Z. Chen, A novel Gaussian process regression model for state-of-health estimation of lithium-ion battery using charging curve, J. Power Sources (384) (2018) 387–395.

[26] C. Ephrem, P. Kollmeyer, M. Preindl, R. Ahmed, A. Emadi, Long short-term memory-networks for accurate state of charge estimation of li-ion batteries, IEEE Trans. Indust. Electron. 67 (7) (2018) 5695–5705.

[27] Y. Zhang, R. Xiong, H. He, M. Pecht, Long short-term memory recurrent neural network for remaining useful life prediction of lithium-ion batteries, IEEE Trans. Veh. Technol. 67 (7) (2018) 5695–5705.

[28] F. Karim, S. Majumdar, H. Darabi, S. Chen, Lstm fully convolutional networks for time series classification, IEEE Access (2017) 1–7.

[29] F. Karim, S. Majumdar, H. Darabi, S. Harford, Multivariate LSTM-FCNs for time series classification, Neural Netw. 116 (2019) 237–245.

[30] B. Bole, C.S. Kulkarni, M. Daigle, Randomized battery usage data set, NASA Ames Progn. Data Repos. (2014).

[31] R.B. Christoph, Diagnosis and Prognosis of Degradation in Lithium-Ion Batteries, Ph.D. Thesis Department of Engineering Science, University of Oxford, Oxford, UK, 2017.

[32] J.L. Elman, Finding structure in time, Cogn. Sci. 14 (1990) 179–211.

[33] Y. Bengio, P. Simard, P. Frascondi, Learning long-term dependencies with gradient descent is difficult, IEEE Trans. Neural Netw. 5 (2) (1994) 157–166.

[34] K. Fukushima, Neocognitron, Scholarpedia 2 (1) (2007) 1717.

[35] Y. LeCun, Y. Bengio, G. Hinton, Deep learning, Nature 521 (2015) 436–444.

[36] F. Karim, S. Majumdar, H. Darabi, S. Chen, Lstm fully convolutional networks for time series classification, IEEE Access (2017) 1–7.

[37] F. Karim, H.Darabi S.Majumdar, S. Harford, Multivariate LSTM-FCNs for time series classification, Neural Netw. 116 (2019) 237–245.

[38] Z. Zhao, Y. Zheng, Z. Zhang, H. Wang, Y. Zhao, Exploring spatio-temporal representations by integrating attention-based bidirectional-LSTM RNNs and FCNs for speech emotion recognition, Proc. Interspeech (2018) 272–276, https://doi.org/10.21437/Interspeech.2018-1477.

[39] D.P. Kingma, J. Ba.Adam, A Method for Stochastic Optimization, Proceedings of the 3rd International Conference on Learning Representations (ICLR), 2014.

[40] H. Zhang, Q. Miao, X. Zhang, Z. Liu, An improved unscented particle filter approach for lithium-ion battery remaining useful life prediction, Microelectron. Reliab. (81) (2018) 288–298.

[41] D. Liu, X. Yin, Y. Song, W. Liu, Y. Peng, An on-line state of health estimation of lithium-ion battery using unscented particle filter, IEEE ACCESS (6) (2018) 40990–41001.

[42] W Yan, B. Zhang, G. Zhao, S. Tang, G. Niu, and X. Wang. Battery management system with Lebesgue sampling-based extended Kalman filter. IEEE Trans. Indust. Electron., 66(4): 3227-3236.

[43] M. Neumann S. Huang, D.E. Marthaler, K. Kersting, pyGPs – A python library for gaussian process regression and classification, J. Machine Learn. Res.. J. Machine Learn. Res. 16 (2015) 2611–2616.